JOURNAL OF MATERIALS SCIENCE 33 (1998) 3541–3553

Aligned microstructure of some particulate polymer composites obtained with an electric field

C. PARK, R. E. ROBERTSON*
Macromolecular Science and Engineering Center and Department of Materials Science and Engineering, The University of Michigan, Ann Arbor, MI 48109, USA
E-mail: rer@umich.edu

Alignment by an electric field was obtained for a variety of particles dispersed in photopolymerizable fluids. The particle shapes studied were irregular, spherical, rhombohedral, rod-like (fibres), and platelet. The sizes ranged from sub-micrometres to tens of micrometres, and the dielectric constants of the particles varied from less than that of the liquid matrix to very much greater than that of the matrix. Polymerization or hardening of the matrix was possible at room temperature, required only a few seconds, and the aligned structures obtained were able to be examined by both light and scanning electron microscopy after fracture or sectioning. Nominally equiaxed particles, containing a statistical proportion of non-equiaxed particles, could be completely aligned at 48 vol % concentration in a fluid having a viscosity of about 2.5 Pa s, but at 57 vol %, the mixture behaved as a paste, and only particle rotation and local rearrangements were possible. The rate of alignment seemed to depend generally on the magnitude of $\varepsilon_1(a\beta)^2$, where ε_1 is the relative dielectric constant of the liquid resin, a is the particle radius, and β is the particle dipole coefficient given by $(\varepsilon_2 - \varepsilon_1)/(\varepsilon_2 + 2\varepsilon_1)$, where ε_2 is the relative dielectric constant of the particles. $\varepsilon_1(a\beta)^2$ emphasizes the importance of particle size and the relative unimportance of the particle dielectric constant for alignment, except when $\varepsilon_2 \approx \varepsilon_1$. Platelets were more rapidly aligned than fibres. © *1998 Kluwer Academic Publishers*

1. Introduction

Particles in a fluid medium under an electric field experience polarization, thermal agitation, hydrodynamic drag, gravity, and colloidal forces. If the polarization force is dominant, the particles are expected to align along the electric field [1]. Particle alignment by an electric field has been reported for many electrorheological fluid systems [2–10], and some workers have suggested that particle alignment is a prerequisite to achieve the electrorheological effect [2, 3, 6–10], though this has been questioned by others [11].

To date, however, few observations have been made of field-induced aligned structures because of the difficulty of observing them directly. Most previous observations of field-induced aligned structures have been limited to optical observations of thin layers that are confined between glass plates [2–4, 7–9, 12–15]. Such systems give only an imperfect representation of an actual three-dimensional system, and the low resolution of optical observations does not allow structures of sub-micrometre particles at high concentration to be observed. Various optical probes have been used to characterize the three-dimensional structure, including light scattering [16], laser diffraction [17], and laser diffuse transmittance [18]. These methods have many restrictions, however, such as the need for a refractive index match between the fluid and particles and low particle concentration. A number of computer simulations of the three-dimensional structure have been also reported [19–25].

In the present work, observations are reported of the three-dimensional structure of the aligned particles under electric fields [26]. This was done by using a photopolymerizable monomer as the fluid. The fluid can be quickly solidified by light without heating while the particulate composite is under the electric field. In addition, the viscosity of the photopolymerizable fluid can be varied, though for the examples described in the present work, the viscosity was kept fairly high ($\approx$2.5 Pa s) to slow particle motion and reduce sedimentation. For study by optical microscopy, the solidified composite can then be sectioned into thin layers at any angle with respect to the alignment axis. For study by scanning electron microscopy, surfaces can be obtained by fracturing the composite

* Author to whom all correspondence should be addressed.

TABLE I Specification and alignment of the inclusions

Inclusion	Size (μm) (diameter)	Shape	Size distribution	Dielectric constant
Silica–zirconia (P50)	1.7	Angular	Broad	3.5
Silica–zirconia (Z100)	0.7	Round	Broad	3.5
Glass sphere	11 or 18	Sphere	Broad	6.9
Glass sphere	25	Sphere	Narrow	6.9
Hollow glass sphere	40	Sphere	Broad	≈1
Glass fibre	180/18 (l/d)[a]	Fibre	Broad	6.6
Hollow glass fibre	200/11 (o.d.[b])/ 5.9 (i.d.[c])	Hollow fibre	Broad	3.9
Aluminosilicate	2.0	Rhombohedron	Narrow	n/a
Barium titanate	1.2	Round	Narrow	2000
Mica	60/20/1.0 ($l/w/t$)[d]	Platelet	Broad	400

[a] Length/diameter.
[b] Outer diameter.
[c] Inner diameter.
[d] Length/width/thickness.

or by polishing sections. The use of a polymerizable fluid was previously described by Randall *et al.* [27–29], though to solidify the fluid, it was heated to a high temperature, which can disturb the alignment. The present report describes the behaviour of a number of particles, which are listed in Table I, and these have allowed an assessment of how the aligned structure is affected by the particle size, size distribution, shape, concentration, and dielectric constant.

2. Experimental procedure

2.1. Materials

Urethane dimethacrylate (UDMA) from Esschem Co. was used as the principal matrix fluid. This was usually mixed with 1,6-hexanediol dimethacrylate (HDDMA), often in a 90/10 ratio, which gave a viscosity that allowed particle alignment to occur in a conveniently observable time range.

To solidify the fluid rapidly, camphorquinone and *N*,*N*-dimethylaminoethyl methacrylate were used as the photosensitive initiator and accelerator, respectively. The chemical structures of these materials are shown in Fig. 1.

Several types of inclusion were used. The most studied inclusion was silica–zirconia ($\approx 96\,SiO_2 \cdot 4ZrO_2$), which was obtained from the 3M Co. in two forms: P50, having an average particle diameter of 1.7 μm, and Z100, having an average particle size of 0.7 μm. Both had broad size distributions. The shape of the typical P50 particle was angular; that of the typical Z100 particle was approximately round.

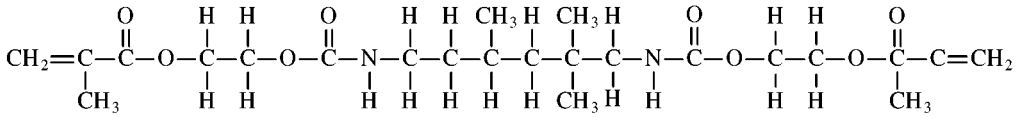

Urethane dimethacrylate

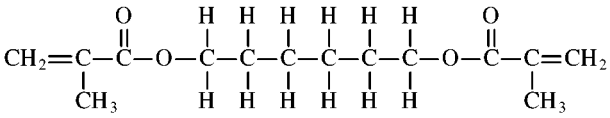

1,6-Hexandiol dimethacrylate

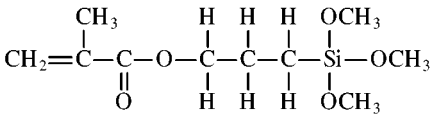

3-Methacryloxypropyltrimethoxy silane

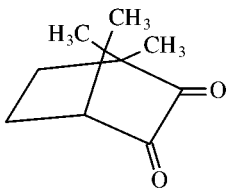

Camphorquinone

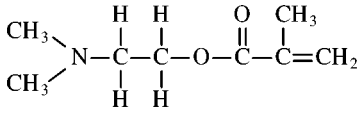

N,N-dimethylaminoethyl methacrylate

Figure 1 Chemical structure of the resin material.

The surfaces of the silica–zirconia were treated with a coupling agent, 3-methacryloxypropyltrimethoxy silane. Another type of inclusion was glass spheres, which were used in three forms: spheres having a narrow size distribution and an average diameter of 25 μm, and spheres having a broad size distribution with the two average diameters of 11 and 18 μm. Equiaxed rhombohedral aluminosilicate particles, barium titanate particles, hollow glass spheres, glass fibres, hollow glass fibres, and mica platelets were also used (see Table I).

2.2. Procedures

UDMA/HDDMA (90/10) resin was prepared as a photopolymerizable fluid with 0.2 wt % initiator and 0.3 wt % accelerator. The inclusions were usually dried in an oven overnight at 105 °C before being dispersed in the fluid. The inclusion concentration was varied from 10–77 wt %. After the inclusions were uniformly mixed with the photopolymerizable fluid, the dispersion was placed in rectangular cuvet cells. To eliminate voids, the cuvet cells were vibrated as they were being filled. For highly concentrated suspensions, the cuvet cells were centrifuged briefly under a centrifugal force of about 250 N in an IEC HN-SII centrifuge.

Aluminium plates were used as electrodes, and the spacing between them was about 7.5 mm. High electric fields (60 Hz a.c. or d.c.) of up to 1.2 kV mm^{-1} were applied to the dispersion in the cuvet cells.

The fluid matrix was polymerized by a blue light gun (Caulk Dentsply) while the electric field was being applied or immediately after the field had been reduced or removed. Under the illumination, the resin gelled to a depth of 3 mm within about 3 s. During the polymerization of the resin, heat was generated at the rate of about 1 °C s, so that the resin could be solidified before the temperature rose about 30 °C, starting at room temperature. A schematic drawing of the experimental apparatus for this is shown in Fig. 2.

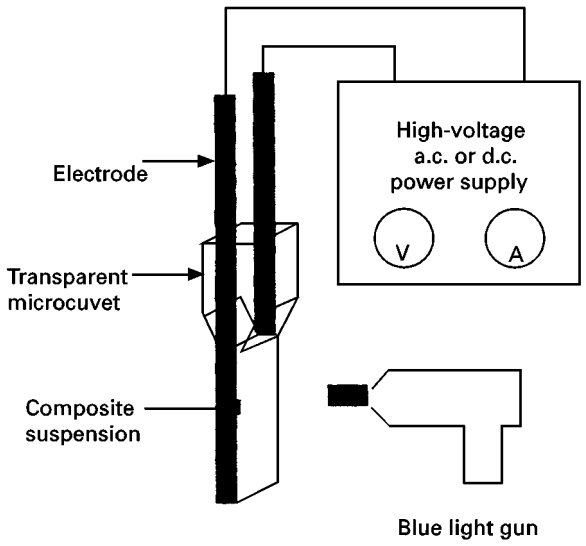

Figure 2 Schematic drawing of the experimental apparatus.

After the light cure, the cured suspensions were placed in an oven at 105 °C for 1 h as a postcure, to complete the reaction and eliminate any residual monomer.

Various types of specimens were prepared for observation from the hardened composites. Thin sections (about 150 μm thick) were obtained by cutting the composite at various angles with respect to the alignment axis with a Buehler Isomet low-speed saw, and these were studied with an Olympus BH-2 transmission optical microscope. Fracture surface specimens were obtained by cleaving the composites after notching with a razor blade. The fractures were initiated both parallel and perpendicular to the electric field direction, both with the plane of the fracture parallel to the electric field. Also, polished sections of the composites, obtained by sectioning both parallel and perpendicular to the electric field and using a 0.05 μm alumina suspension for the final stage of polishing, were studied. The fracture and polished surfaces were examined with a Hitachi S-800 scanning electron microscope (SEM).

3. Results

A concise description of the inclusions studied is given in Table I. All of these could be aligned parallel to the electric field, though not all to the same degree.

3.1. Silica–zirconia

Good Alignment of the silica–zirconia particles into strings was obtained between the electrodes with both a.c. and d.c. fields. The a.c. field usually produced the better alignment because electrophoresis was absent. At high particle concentrations, however, the particles no longer formed distinct strings, but the structure still appeared more ordered than that not subjected to an electric field. The alignment was examined both by fracturing and by cutting and polishing specimens after the matrix had been hardened.

3.1.1. Fracture surfaces

Fracture surfaces were prepared by fracturing along and across the alignment direction on planes parallel to the alignment axis. Examples of scanning electron micrographs of these two types of specimen are shown in Fig. 3. The most distinctive features in the micrographs in Fig. 3 are the crack bifurcation lines. These are steps in elevation on the surface, and their distinctiveness arises from the white glow of the sharp step edges. The bifurcation lines on the surfaces obtained by fracturing parallel to the electric field (Fig. 3a) were much longer than those obtained by fracturing perpendicular to the field (Fig. 3b). Also, the bifurcation lines parallel to the electric field increased in length with increase in field strength, but those perpendicular to the electric field tended to be constant in length, independent of field strength. The latter bifurcation lines were usually limited by the separation between particle strings lying on the surface, though the density of bifurcation lines and the lateral extent of the groups of aligned points at which

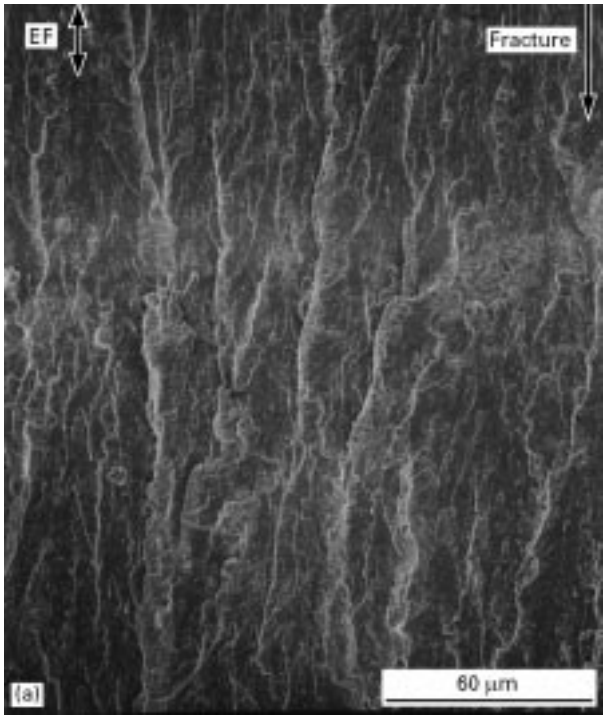

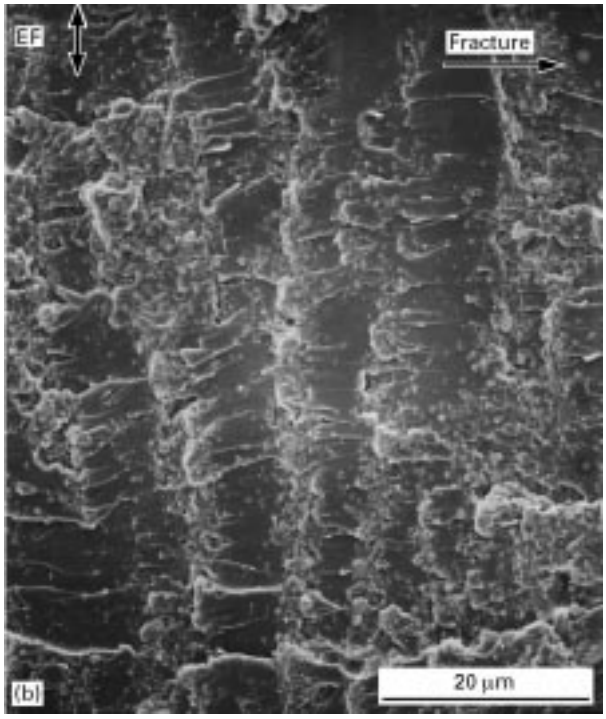

Figure 3 Scanning electron micrographs of aligned silica–zirconia (P50) composite (29 vol %) fractured (a) parallel and (b) perpendicular to the electric field. Polymerized after 1 min under 1 kV mm^{-1} a.c.

bifurcation lines initiated during perpendicular fracture, did increase with increasing electric field strength.

The length of the bifurcation lines from fracture parallel to the electric field and the length of the aligned loci of bifurcation points from fracture perpendicular to the field, each taken from high magnification scanning electron micrographs, can both be used as measures of the string length. The two lengths are not the same, nor does either usually give the actual string length. The length of the bifurcation lines

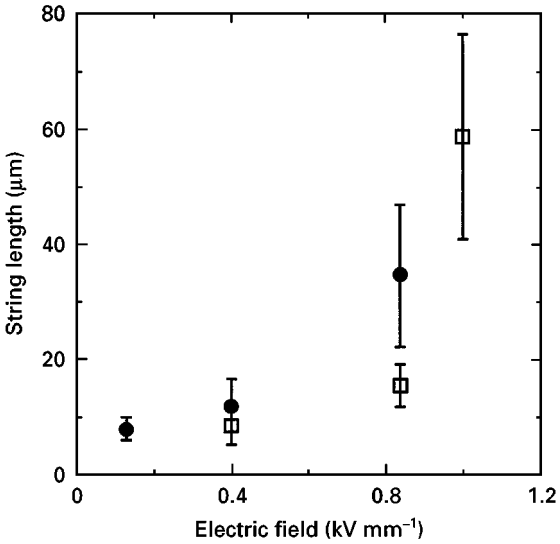

Figure 4 String length of aligned silica–zirconia (P50) composite (29 vol %) versus electric field after 1 min. (●) Fractured parallel, (□) perpendicular to the field direction.

from fracture parallel to the electric field tends to overestimate the string length, because the bifurcation lines tend to continue after the string has ended. The length of the aligned loci of points at which bifurcation lines initiated from fracture perpendicular to the field tends to underestimate the string length, because the fracture plane and the plane in which the string resides may not be coincident for the full length of the string.

An example is shown in Fig. 4 of the string length after 1 min as represented by these two measures versus applied electric field strength. The string length is seen to increase more rapidly than linearly with electric field for each of them. In contrast, at fixed field strength, the string length increases linearly with time for short times [26].

For fracture parallel to the alignment axis, the bifurcation lines often arise as grooves or the edges of grooves that have resulted from the removal of whole aligned strings. An example with 50 wt % (29 vol %) silica–zirconia (P50), is shown in Fig. 5. The P50 particles were about 1.7 μm in diameter. Although the reinforcing effect of aligned particles is not like that of fibres, the aligned strings seem to behave like short fibres with respect to their effect on fracture parallel to the alignment axis.

3.1.2. Polished surfaces

Although the fracture surface morphology gives a good view of the structure at low concentrations of particles, the structure at high concentrations becomes too complicated for easy study even with scanning electron microscopy. But polished surfaces, which give clear boundaries between particles in a string or column, continue to allow details of the aligned structure to be discerned. Two kinds of polished surfaces were prepared: parallel to the electric field and perpendicular to the field.

An example of the structure seen by cutting and polishing a specimen parallel to the field direction is

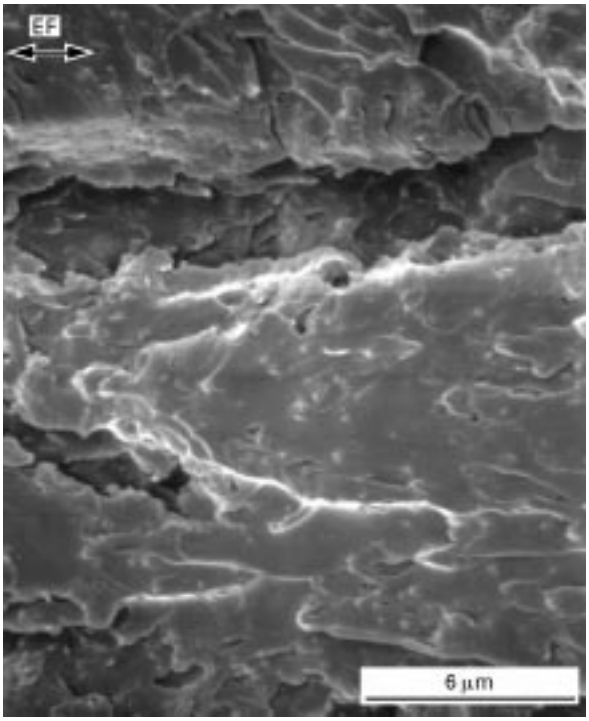

Figure 5 Scanning electron micrographs of aligned silica–zirconia (P50) composite (29 vol %) fractured parallel to the electric field (grooves). Polymerized after 1 min under 1 kV mm^{-1} a.c.

shown in Fig. 6. This specimen contained 50 wt % (29 vol %) silica–zirconia (P50), and it had been cured after applying a field of 1 kV mm^{-1} a.c. for 1 min. The string widths are seen to be mostly determined by the diameters of the largest particles in the strings. One can notice from Fig. 6 how well angular-shaped particles are able to pack under the stimulus of the electric field. The longest axis of each particle tends to become aligned with the field, and the particles seem also to have rotated about these axes to fit even better together with their neighbours. Also seen in Fig. 6b are the many small particles (<0.4 μm diameter) that were not aligned in the strings but remained dispersed in the matrix between the strings. Although the fine particles may eventually join the strings, the entire structure usually will have become more complex by then.

At high particle concentrations, the nature of the alignment changed from that at lower concentrations. As seen in Fig. 7, strings are still discernible with 70 wt % (48 vol %) P50, but are much less so with 77 wt % (57 vol %) Z100, and even with 70 wt % (48 vol %) P50, the alignment is not as regular as that with lower particle concentrations. With 77 wt % (57 vol %) Z100, which has the consistency of a paste, alignment has mostly involved local rearrangement and rotation of the particles. Still, this allows the structure to become obviously different from the structure not exposed to an electric field.

3.1.3. String cross-section

Typical cross-sections perpendicular to the alignment axis for a medium filler loading are shown in Fig. 8. Two particle types are represented in Fig. 8a and b: round (Z100) and angular (P50), respectively. Both

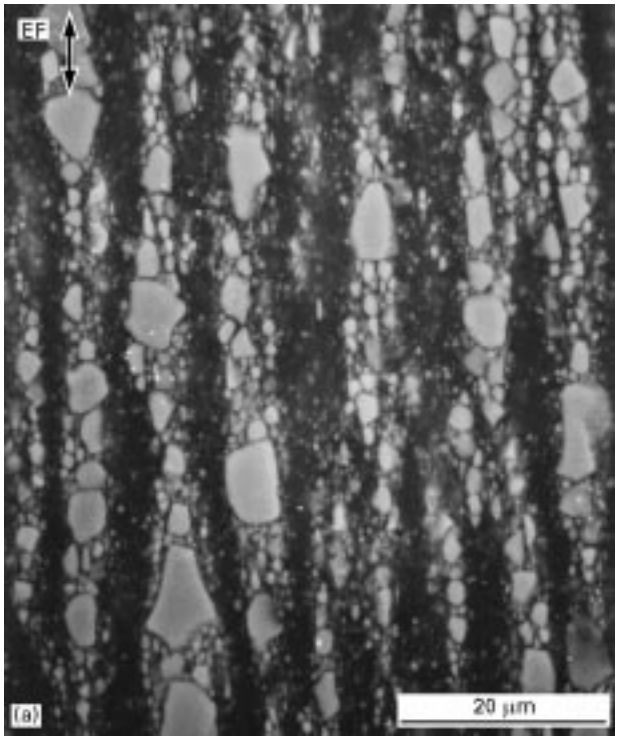

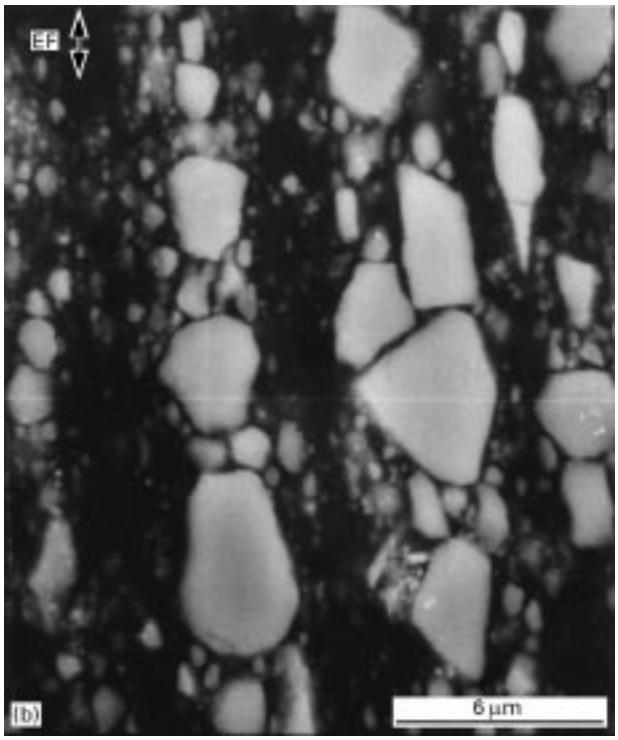

Figure 6 Scanning electron micrographs of aligned silica–zirconia (P50) composite (29 vol %) sectioned and polished parallel to the electric field, polymerized after 1 min under 1 kV mm^{-1} a.c.

particles have aspect ratios greater than one, as can be seen in Figs 7b (Z100) and 6b (P50). As seen in Fig. 8a, after 1 min at 1 kV mm^{-1} a.c., the larger particles tended to be equidistant from one another, except within the agglomerate (centre right), and to appear to be nearly round in this view. These larger particles represent the strings. Without alignment, the particles in such a cross section appear to be less uniformly distributed and less round. After a longer alignment time (10 min at 1 kV mm^{-1}), an example of which is

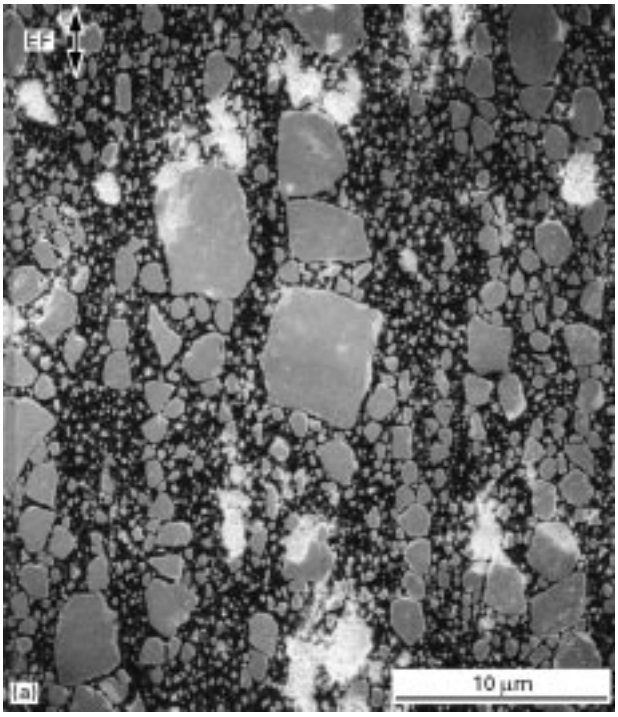

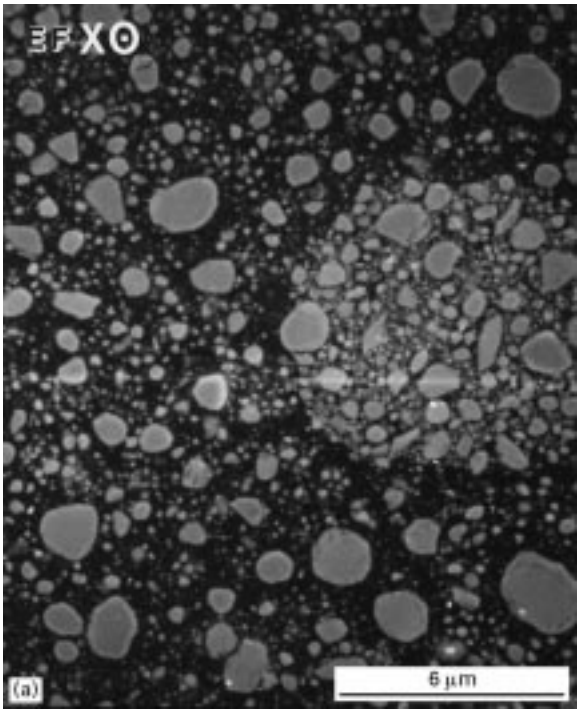

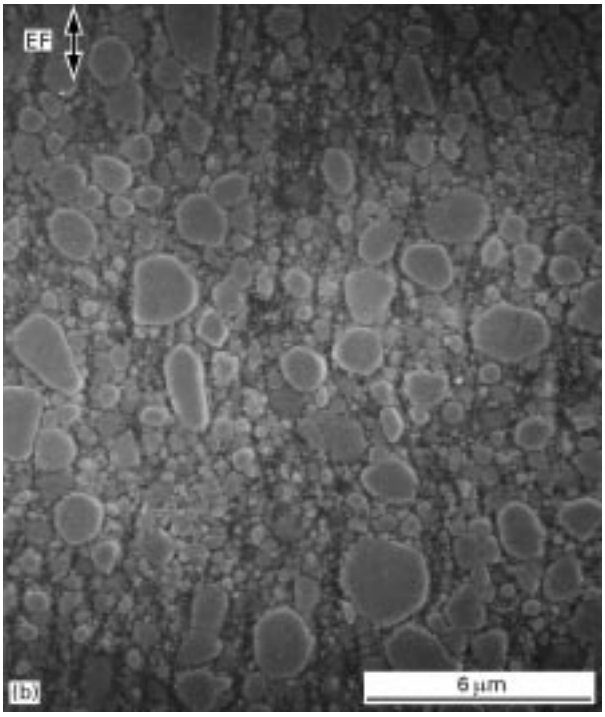

Figure 7 Scanning electron micrographs of aligned silica–zirconia composites sectioned and polished parallel to the electric field: (a) 48 vol % P50 and (b) 57 vol % Z100, polymerized after 30 s under 1.2 and 0.8 kV mm^{-1} a.c., respectively.

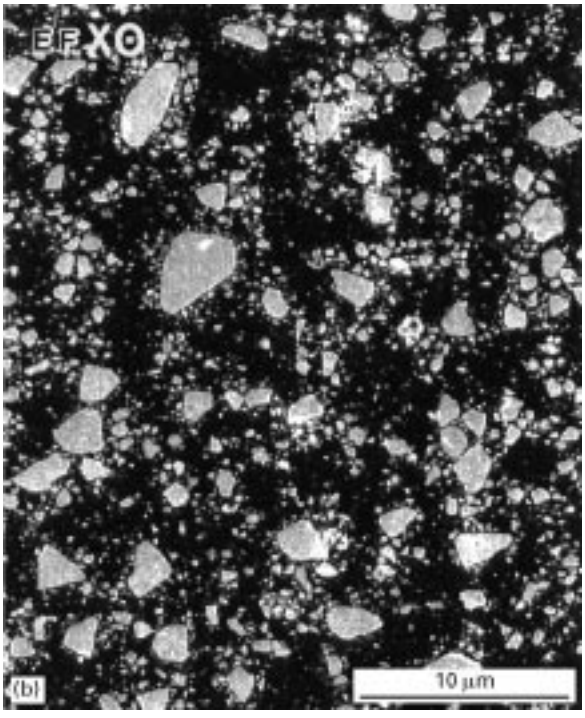

Figure 8 Scanning electron micrographs of aligned silica–zirconia composites sectioned and polished perpendicular to the electric field: (a) 37 vol % Z100, polymerized after 1 min and (b) 29 vol % P50, polymerized 10 min under 1 kV mm^{-1} a.c.

shown in Fig. 8b, the structure became more complex. Many of the larger particles have become more equidistant from their neighbours and rounder appearing. But for others, coalescence of the strings has begun. Also, these larger particles (strings) tend to be surrounded by swarms of smaller particles, with a depletion of particles further away from the strings.

3.1.4. Agglomerates

Although attempts were made in the preparation of the mixtures of particles and liquid matrix resin to keep agglomerates to a minimum, they were present in the specimens, and they were also observed to align with the electric field. The alignment of an agglomerate in a 50 wt % (29 vol %) silica–zirconia (P50) polished specimen is shown in Fig. 9. The aggregate is distinguishable by its having a higher particle density than the surrounding area and lacking particle strings. In contrast to the elongation of the aggregate in the field direction, in cross sections normal to the alignment axis, as seen in Figs 8a and 10, the aggregate tended to be round. In addition, the larger non-equiaxed particles within the aggregate seem to have

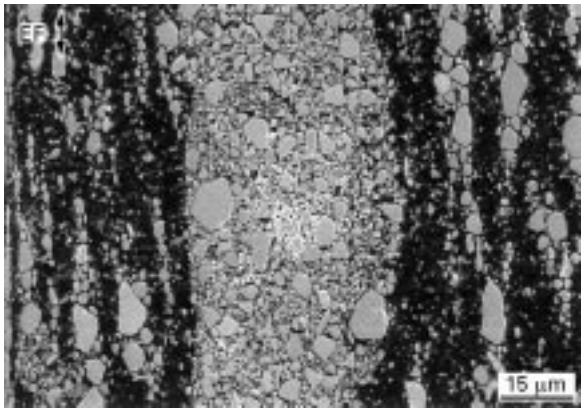

Figure 9 Scanning electron micrographs of aligned silica–zirconia (P50) composite (29 vol %) sectioned and polished parallel to the electric field, showing an aligned agglomerate. Polymerized after 1 min under 1 kV mm^{-1} a.c.

been able to rotate so that their longest axis was aligned with the field, and the aggregate as a whole may even have been elongated by the field. The edge of one of the agglomerates, sectioned perpendicular to the field, is shown at higher magnification in Fig. 10b, and the agglomerate is seen to be surrounded by a thin layer of resin that is largely depleted of particles. (These resin bands have allowed the agglomerates in Fig. 10a to become visible.) The thickness of the resin layer ranged from 1–3 μm. The more concentrated the particles in the agglomerate, the thicker the resin layer, suggesting that the resin had been squeezed from the aggregate as the particles within it had been drawn together by the field.

3.2. Glass spheres

A simpler system to analyse than the above is a dispersion of spheres. Glass spheres with a narrow size distribution and an average diameter of approximately 25 μm were studied. These relatively large spheres allowed the details of the structure to be observed at low concentrations, and they aligned much faster than did the silica–zirconia particles, forming an excellent aligned structure. An example at 10 vol % aligned with an electric field of 0.9 kV mm^{-1} a.c. is shown in Fig. 11. Fig. 11a–d show the alignment of the particles after the field was applied for 1, 10 s, 1 and 4 min, respectively. (At the end of these times, the field was removed or reduced and the matrix resin photopolymerized, which took a few seconds.) Most of the particles attached to one another in groups of two to four within 1 s, but these groupings had not yet completely aligned parallel with the applied field. After 10 s, most of the particles had joined into linearly aligned strings. Most of the strings were composed of a single row of particles. After 1 min, the string length had almost doubled and slight coarsening had started to occur, with the coalescence of strings to form columns. A higher magnification inset in Fig. 11c shows the tendency for the strings to nest within one another as they coalesce to form a column. After 4 min, some of the string columns spanned the entire separation between the electrodes.

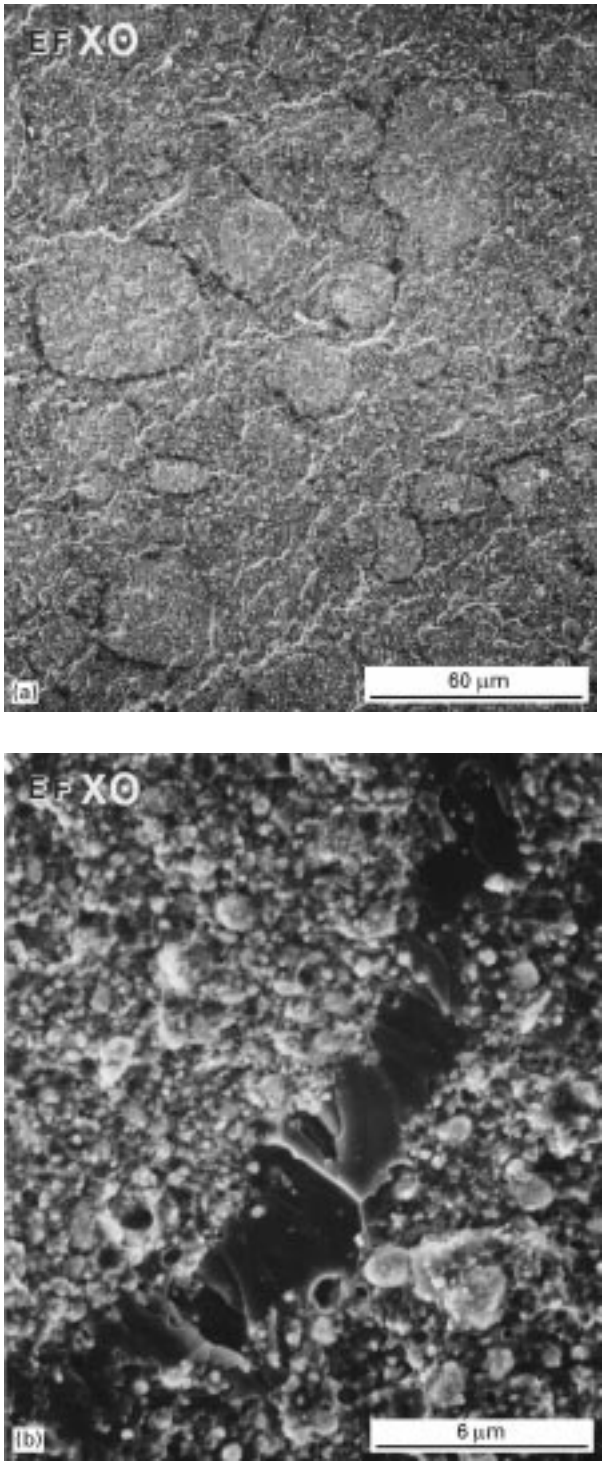

Figure 10 Scanning electron micrographs of aligned silica–zirconia (Z100) composite (37 vol %) sectioned and polished perpendicular to the electric field. Polymerized after 1 min under 1 kV mm^{-1} a.c.

With further field application time, the strings continued to join and coarsen.

Broad size distributions of glass spheres averaging 11 and 18 μm diameter were also studied, and these also aligned well, though not as well as the narrow size distribution. Fig. 12 shows the fracture surface of a composite with 20 vol % glass spheres averaging 11 μm in diameter. The string length increased with field application time, and the quality of the alignment increased with field strength up to 0.80 kV mm^{-1}, beyond which no further increase in alignment occurred. The thickness of the strings was not uniform, and

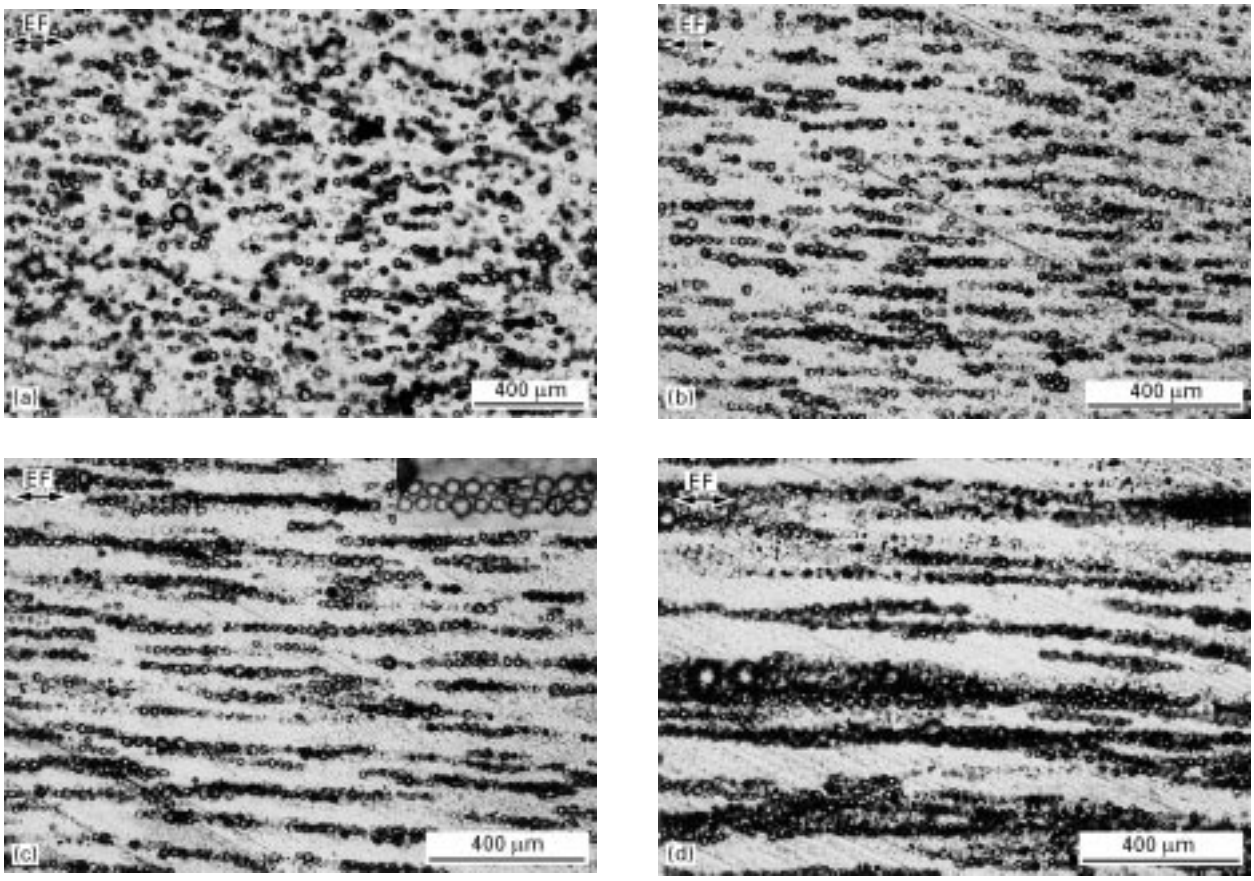

Figure 11 Optical micrographs of thin sections containing 10 vol % aligned glass spheres having a narrow size distribution, polymerized after (a) 1 s, (b) 10 s (c) 1 min, and (d) 4 min under 0.9 kV mm^{-1} a.c. (The inset in (c) shows details of a pairing of strings.)

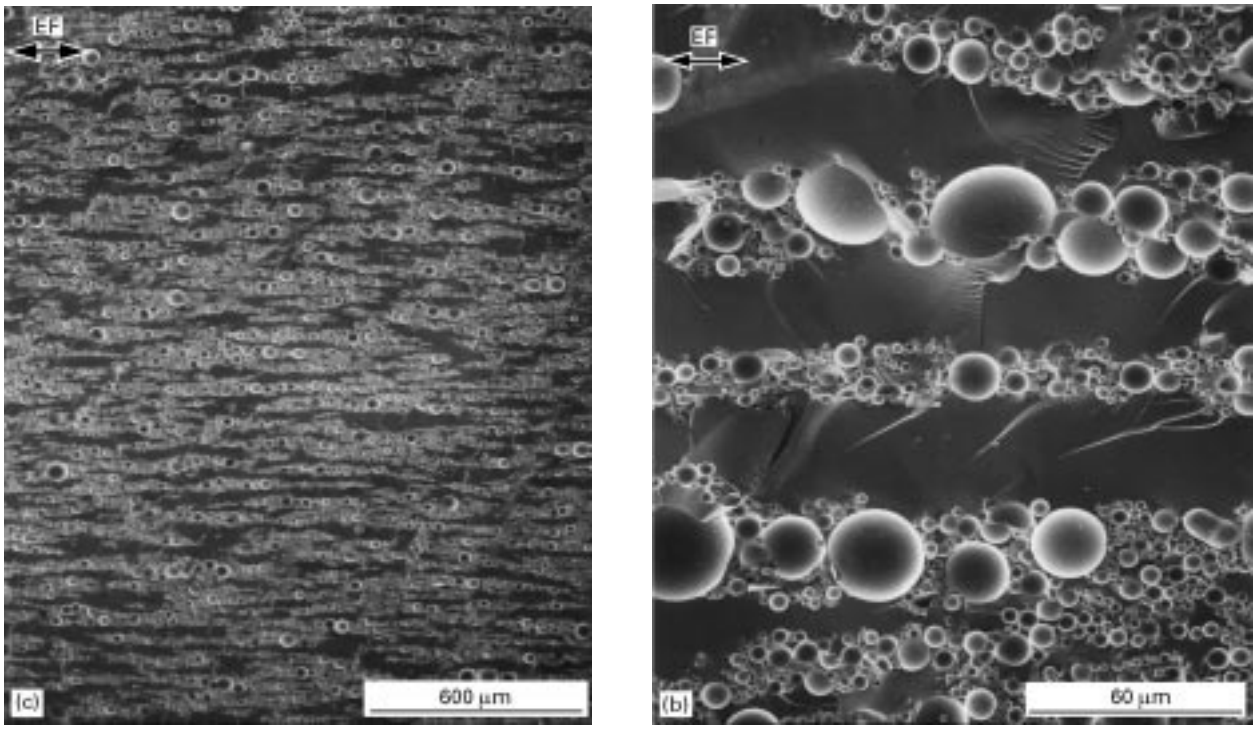

Figure 12 Scanning electron micrographs of aligned glass spheres (20 vol %) having a broad size distribution, polymerized after 5 min under 0.6 kV mm^{-1} a.c.

this became especially so as the strings grew by the coalescence of neighbouring strings. Before coalescence, the strings tended to be the width of the largest spheres within them. Along side these spheres, enough smaller particles tended to congregate to continue the same width. Coalescence tended to disrupt the alignment, producing what appeared to be angular bends in the string.

3.3. Hollow glass spheres

Excellent alignment was also obtained with 38 vol % hollow glass spheres dispersed in the same matrix resin. An example is shown in Fig. 13a. Hollow glass spheres have a lower bulk dielectric constant than does the resin. After several minutes under 0.8 kV mm^{-1} a.c., the particles had moved away from both electrodes, leaving pure resin layers near the electrodes. This was presumably caused by dielectrophoresis. An example of this after 4.5 min is shown in Fig. 13b, showing the particles strings at the boundary of the particle-depleted resin.

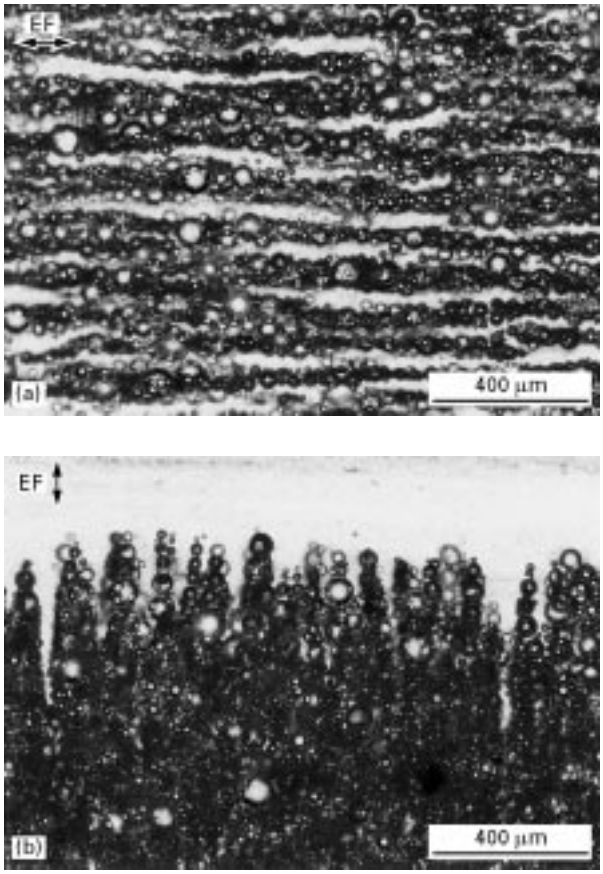

Figure 13 Optical micrographs of thin sections of aligned hollow glass spheres (38 vol %): polymerized after (a) 30 s and (b) 4.5 min under 0.8 kV mm^{-1} a.c.

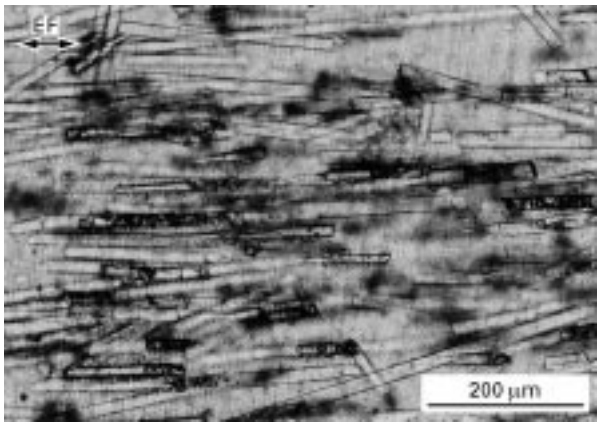

Figure 14 Optical micrographs of a thin section of aligned glass fibres (4.5 vol %), polymerized after 30 s under 0.8 kV mm^{-1} a.c.

3.4. Glass fibres

Both solid and hollow fibers were aligned parallel to the electric field, but fibres for which the initial orientation was nearly perpendicular to the electric field before the field was applied tended to move sluggishly, and their alignment was often incomplete. An example of the solid fibre alignment is shown in Fig. 14 after a 30 s application of an a.c. field of 0.81 kV mm^{-1}. A major contributor to the sluggishness was the small aligning moments for nearly perpendicularly oriented fibres. But the hydrodynamic resistance to rotation was also a factor. Although the aligning forces were greater for longer fibres, shorter fibres usually aligned more rapidly.

3.5. Aluminosilicate particles

In contrast to most of the other particles in this study, the best alignment with the aluminosilicate particles was obtained with a d.c. field. Scanning electron micrographs of fracture surfaces of specimens containing 5.4 vol % aluminosilicate particles showing excellent alignment under a d.c. field are seen in Fig. 15. The rhombohedral particles tended to align in the strings along their diagonals and were packed very efficiently. Most of the particles joined strings within one minute. The strings were thicker than a single particle width, and narrow necks were frequently observed. Also, thin regions of resin largely depleted of particles were found within the thick string column (see Fig. 15b). Possibly several thin strings formed earlier had coalesced to coarsen the strings before the matrix was solidified.

3.6. Barium titanate

Excellent alignment of barium titanate was obtained with the relatively low electric field of 0.27 kV mm^{-1} a.c. in spite of the small size (1.2 μm) of the particles. There was no noticeable alignment at 1 s, but most of the particles had joined into short strings within 30 s. Because the particles have a non-equiaxed granular shape, the strings that formed tended to be irregular with non-uniform thickness. The strings became longer with continued field application. Aggregation of the strings and coarsened columns were often observed at 5 min. This alignment sequence is shown in Fig. 16 as a series of micrographs of fracture surfaces obtained by fracturing perpendicular to the alignment axis in the plane of the axis. The surfaces show that the number of the bifurcation lines increased markedly with alignment. (Compare Fig. 16a with the other three micrographs in Fig. 16.) Also, the bifurcation lines in the more fully aligned composites (Fig. 16c and d) suggest that the crack was arrested at each of the strings and the bifurcation lines then had to reinitiate. In spite of the reinitiation at each string, the separation between bifurcation lines remained relatively constant at about 10 μm, giving a scale-like appearance. The constant separation suggests a relatively uniform separation of about 10 μm between the strings.

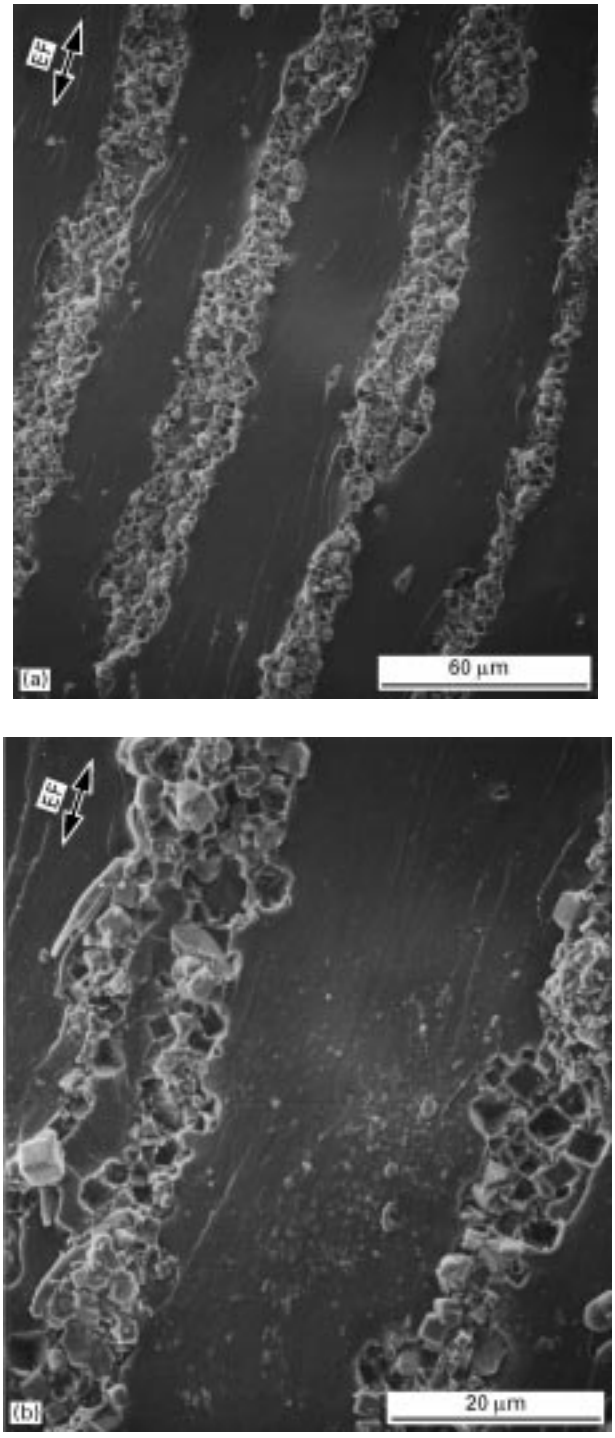

Figure 15 Scanning electron micrographs of aligned aluminosilicate particles (5.4 vol %), polymerized after 1 s under 0.8 kV mm^{-1} d.c.

3.7. Mica

Mica platelets (length/width/thickness = 60/20/1) having an aspect ratio in the platelet plane of 3 : 1 aligned with the electric field very rapidly. Most of the platelets were individually aligned within 1 s at 1.0 kV mm^{-1} a.c., and the alignment was essentially complete within 7 s, with no further change being observed in the structure as the field was continued to be applied for a total of 10 min. There was no migration of the aligned platelets to form larger structures. Neither linear strings nor columns were formed during the 10 min field application. Examples of optical micrographs of the platelet alignment after 7 s and 10 min under 1.0 kV mm^{-1} are shown in Fig. 17.

4. Discussion

Alignment by an electric field was obtained for a variety of particles dispersed in photopolymerizable fluids. The particle shapes were irregular, spherical, rhombohedral, rod-like (fibres), and platelet. The sizes ranged from sub-micrometres to tens of micrometres, and the dielectric constants of the particles varied from less than that of the liquid matrix to very much greater than that of the matrix. All of the strings that formed, whether from silica–zirconia particles, glass spheres, aluminosilicate particles, or barium titanate particles, large or small, broadly or narrowly distributed in size, were compact. The rhombohedral aluminosilicate particles, all having similar shapes and aligned along their diagonals, were able to nest, as can be seen in Fig. 15b. The spherical particles, though unable to nest, formed strings of very uniform diameter when the spheres were of the same size, and the spherical particles having a broad size distribution formed compact strings or columns by the smaller spheres filling in where they could around larger spheres.

Particle alignment was observed with both a.c. and d.c. fields, but at high field strengths, d.c. fields caused electrophoresis. Particle depletion around the cathode and particle accumulation around the anode occurred after several minutes under high d.c. field. Also, the current increased with time, accompanied by increases in temperature and mobility of the charge carriers. Electrophoresis was least severe with aluminosilicate particles, though it became significant at higher field strengths (>2 kV mm^{-1}). To prevent electrophoresis, a 60 Hz a.c. field was used for the alignment of all particles except the aluminosilicate.

4.1. Size, size distribution, and shape

The field-induced polarization force, caused by a mismatch between the two phases in dielectric constant (for a.c.) or conductivity (for d.c.) [30], is the driving force for alignment of inclusions in a medium under an electric field. Acting against this at low particle concentration, is the misaligning thermal forces from Brownian motion [1]. To achieve alignment, the aligning forces should be larger than the misaligning forces. This occurs with dissimilar dielectric constant when the dimensionless parameter, λ, which is the ratio of polarization energy to thermal energy [31], is greater than one.

$$\lambda = \frac{\pi\varepsilon_0\varepsilon_1 a^3(\beta E)^2}{k_B T} \tag{1}$$

where ε_0 is the premittivity of free space, a is the radius of the particle, ε_1 is the relative dielectric constant of the liquid resin (about 2.5), E is the applied electric field, k_B is Boltzmann's constant, and T is the absolute temperature. β is the particle dipole coefficient given by $(\varepsilon_2 - \varepsilon_1)/(\varepsilon_2 + 2\varepsilon_1)$, where ε_2 is the relative dielectric constant of the particles.

For all of the inclusions in this study, sufficiently high electric field strengths were able to be applied for the values of λ to be significantly greater than one. The

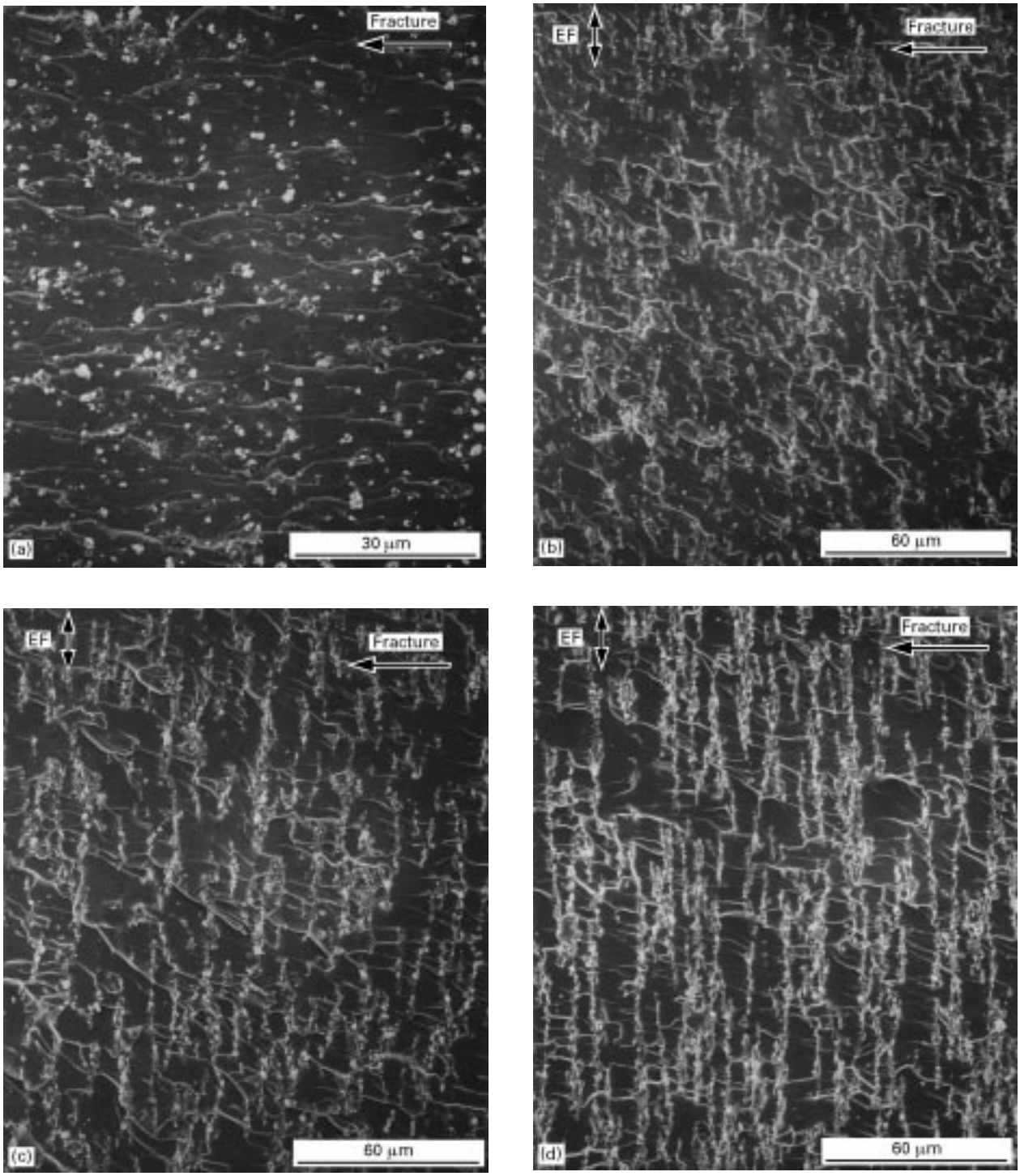

Figure 16 Scanning electron micrographs of aligned barium titanate composite (4.0 vol %), polymerized after (a) no alignment (0 s), (b) 30 s, (c) 60 s, and (d) 300 s under 0.27 kV mm^{-1} a.c.

silica–zirconia and the barium titanate suspensions had the lowest polarization forces in this study, and the values of λ for these suspensions were of the order of 100, considering the average particle size and the magnitudes of the electric fields applied. However, for some of the smaller particles in broad size distributions, $\lambda < 1$. For example, the critical particle radius (for $\lambda = 1$) for silica–zirconia at room temperature and under a field strength of 1.0 kV mm^{-1} was 0.1–0.2 μm. This is consistent with behaviour suggested by Fig. 6b, where many small particles (<0.4 μm diameter) were not aligned.

However, at high particle concentrations and after string and column formation begins, even small particles began to be attracted to the strings. The polarization forces among the inclusions involve multipole interactions [26], and strings and columns seem to exert non-uniform, locally higher polarization forces on their neighbours. The attraction between strings or columns and the smaller particles is seen, for example, in Fig. 8b, by the swarm of small particles around the strings.

Although both the fibres and platelets had similarly high aspect ratios, which might have been expected to

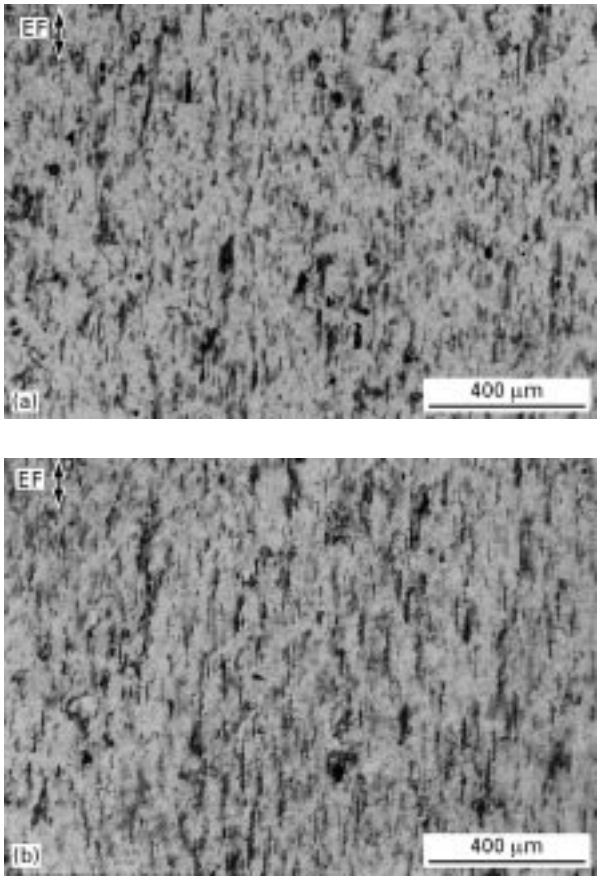

Figure 17 Optical micrographs of thin sections containing aligned mica platelet (4.3 vol %), polymerized after (a) 7 s and (b) 10 min under 1 kV mm^{-1} a.c.

result in similarly high driving forces for alignment with the electric field, the rapidity of their alignment was significantly different. The fibres tended to move sluggishly, and their alignment was often incomplete, unless their axes were initially oriented nearly parallel to the electric field, because of steric interference between the fibres. Platelets, on the other hand, were aligned very rapidly (within 1 s). Part of the difference results from the longer length of the fibres and the higher dielectric constant of mica.

Another reason for the rapid alignment of plates versus that of fibres may be related to differences in their shape. The platelets studied had an aspect ratio in the platelet plane of about three (length/width = 69/20) (Table I), in addition to the length/thickness ratio of 60/1. Thus, to bring the longest axis of the platelets parallel with the field, much of the rotation can occur in the plane of the platelet, for which the drag force is small, due to the small platelet thickness. This mode of rotation depends on the orientation of the normal to the platelet plane with respect to the electric fields, and is most active when the plate normal is perpendicular to the electric field, which happens to be the most likely orientation: the likelihood for the plate normal to be oriented at an angle φ with respect to the electric field axis is proportional to $\sin\varphi$. For fibres, alignment is easiest for those most closely oriented along the field axis, but alignment along this axis is relatively unlikely. The probability of the fibre axis being oriented at the angle φ with respect to an arbitrary axis, like the electric field axis, is also proportional to $\sin\varphi$.

4.2. Concentration

The rate and ultimate degree of alignment were generally independent of concentration at low to moderate concentrations. However, at higher concentration, the rate and degree of alignment were reduced. The critical concentration depended on the particle aspect ratio. For fibres 180 μm long and 18 μm diameter, the critical concentration was below 10 vol %, and this decreased with increasing fibre length. For nominally equiaxed inclusions like the silica–zirconia particles, which still contained a statistical proportion of non-equiaxed particles, the inclusions were mostly able to align at 48 vol %, with the larger particles aligning first. At 57 vol %, for which the suspension was paste-like and did not flow at ambient temperature (22 °C), only some rotation and local rearrangements were possible. Particles with their longest axes close to being perpendicular to the electric field were usually not able to overcome the resistance of their neighbours because of the paucity of unoccupied space.

4.3. Dielectric constant

Barium titanates particles aligned no better than silica–zirconia particles of similar size in spite of barium titanate's high dielectric constant (around 2000). In Equation 1, the particle dipole coefficient β is defined as the relative value $(\varepsilon_2 - \varepsilon_1)/(\varepsilon_2 + 2\varepsilon_1)$ and has the maximum value of 1, which occurs when the dielectric constant for the inclusions becomes infinite. Therefore, the effect of the dielectric constant mismatch on alignment is limited and is usually less critical than that of the inclusion size. For example, the degree of the alignment of barium titanate particles was less good than that of glass spheres, which were an order of magnitude larger in size.

According to Equation 1, the driving force for alignment is proportional to $\varepsilon_1 a^3(\beta E)^2$. Because the hydrodynamic resistance to alignment from the fluid is proportional to a, the rapidity of alignment is expected to be proportional to $\varepsilon_1(a\beta E)^2$. Considering only the material properties, the parameter is $\varepsilon_1(a\beta)^2$. Assuming a dielectric constant of 2.5 for the liquid matrix, in units of 10^{-12} m^2, $\varepsilon_1(a\beta)^2$ equals 0.0043 and 0.025, respectively, for the two silica–zirconia particles, 10.3, 27.7, and 53.4, respectively, for the glass spheres, 62.5 for the hollow glass spheres, and 0.89 for the barium titanate particles. These numbers emphasize the importance of particle size and the relative unimportance of dielectric constant for alignment.

The hollow glass spheres differ from the other particles studied in that their dielectric constant is less than that of the liquid matrix resin. This is indicated also by the exclusion of these spheres from the regions around the electrodes seen in Fig. 13b. Because the glass shell is very thin, we estimate their dielectric constant to be ≈ 1. This estimate is consistent with the above value for the parameter $\varepsilon_1(a\beta)^2$. The

alignment obtained with the hollow glass spheres after 30 s (Fig. 13a) is similar to that obtained with the largest solid glass spheres after 1 min (Fig. 11c). The respective values for the parameter are $6.25 \times 10^{-12}\,m^2$ and $53.4 \times 10^{-12}\,m^2$. Similar good alignment of particles having a lower dielectric constant than the liquid matrix was also seen with polystyrene particles in water [32].

The parameter $\varepsilon_1(a\beta E)^2$ suggests that the rate of alignment increases with the square of the electric field. Ginder has observed that the aggregation time, which is the inverse of the rate of inclusion motion, increased inversely with the square of the a.c. field strength [18]. For fixed field application time, the string length was found to increase more rapidly than linearly with electric field strength (Fig. 4), and though the string length estimated from the bifurcation lines parallel to the electric field seem to depend on the square of the field strength, the grouping of bifurcation lines perpendicular to the field seems to depend more strongly on field strength. Assuming the actual string length is between these, the string length for these particles would seem to increase more rapidly than the square of the field strength. This difference could be related to the particles being angular and non-equiaxed and having a broad size distribution.

5. Conclusions

Particles of different shapes, sizes, and dielectric constants could be aligned in a photopolymerizable fluid by an electric field. After polymerization, the aligned structures could be studied. Nominally equiaxed particles, containing a statistical proportion of non-equiaxed particles, were completely aligned at 48 vol % concentration in a fluid having a viscosity of about 2.5 Pa s, but at 57 vol %, at which concentration the mixture behaved as a paste, only particle rotation and local rearrangements were possible. The rate of alignment seemed generally to depend on the magnitude of the quantity $\varepsilon_1(a\beta)^2$, where ε_1 is the relative dielectric constant of the liquid resin (about 2.5), a is the particle radius, and β is the particle dipole coefficient given by $(\varepsilon_2 - \varepsilon_1)/(\varepsilon_2 + 2\varepsilon_1)$, where ε_2 is the relative dielectric constant of the particles. The quantity $\varepsilon_1(a\beta)^2$ emphasizes the importance of particle size and the relative unimportance of dielectric constant for alignment, except when $\varepsilon_2 \approx \varepsilon_1$. Platelets were more rapidly aligned than fibres.

Acknowledgements

We thank Professor Frank E. Filisko for his help in initiating these experiments. This research was supported by Grant P50-DE09296 from the National Institute of Dental Research, National Institutes of Health, Bethesda, MD 20892, USA.

References

1. H. A. POHL, "Dielectrophoresis: The Behavior of Neutral Matter in Nonuniform Electric Fields" (Cambridge University Press, Cambridge, 1978).
2. W. WINSLOW, *J. Appl. Phys.* **20** (1949) 1137.
3. N. I. GAMAYUNOV and V. A. MURTSOVKIN, *J. Eng. Phys.* **43** (1982) 963.
4. J. E. STRANGROOM, *Phys. Technol.* **14** (1983) 290.
5. A. F. SPRECHER, J. D. CARLSON and H. CONARD, *Mater. Sci. Eng.* **95** (1987) 187.
6. H. BLOCK and J. P. KELLY, *J. Phys. D* **21** (1988) 1661.
7. S. FRADEN, A. J. HURD and R. B. MEYER, *Phys. Rev. Lett.* **63** (1989) 2373.
8. T. C. JORDAN, *IEEE Trans. Elec. Inst.* **24** (1989) 849.
9. D. J. KLINGENBERG and C. F. ZUKOSKI IV, *Langmuir* **6** (1990) 15.
10. H. CONRAD, Y. CHEN and A. F. SPRECHER, in "Proceedings of the International Conference on Electrorheological Fluids", edited by R. Tao (World Scientific, River Edge, 1992) p. 195.
11. D. L. KLASS and T. W. MARTINEK, *J. Appl. Phys.* **38** (1967) 67.
12. J. C. HILL and T. H. VAN STEENKISTE, *ibid.* **70** (1991) 1207.
13. J. E. MARTIN, J. ODINEK and T. C. HALSEY, *J. Coll. Interface Sci.* **167** (1994) 437.
14. T. Y. CHEN, B. J. BRISCOE and P. F. LUCKHAM, *J. Chem. Soc. Farad. Trans.* **91** (1995) 1787.
15. J. M. GINDER and S. L. CECCIO, *J. Rheol.* **39** (1995) 211.
16. J. E. MARTIN, J. ODINEK and T. C. HALSEY, *Phys. Rev. Lett.* **69** (1992) 1524.
17. T. CHEN, R. N. ZITTER and R. TAO, *ibid.* **68** (1992) 2555.
18. J. M. GINDER, *Phys. Rev. E* **47** (1993) 3418.
19. D. J. KLINGENBERG, F. V. SWOL and C. F. ZUKOSKI, *J. Chem. Phys.* **91** (1989) 7888.
20. M. WHITTLE, *J. Non-Newtonian Fluid Mech.* **37** (1990) 233.
21. D. J. KLINGENBERG, F. V. SWOL and C. F. ZUKOSKI, *J. Chem. Phys.* **94** (1991) 6160.
22. R. T. BONNECAZE and J. F. BRADY, *J. Chem. Phys.* **96** (1992) 2183.
23. K. C. HASS, *Phys. Rev. E* **47** (1993) 3362.
24. W. R. TOOR, *J. Coll. Interface Sci.* **156** (1993) 335.
25. J. R. MELROSE and D. M. HEYES, *J. Chem. Phys.* **98** (1993) 5873.
26. C. PARK, PhD thesis, The University of Michigan, Ann Arbor (1997).
27. C. A. RANDALL, S. MIYAZAKI, K. L. MORE, A. S. BHALLA and R. E. NEWNHAM, *Mater. Lett.* **15** (1992) 26.
28. C. A. RANDALL, D. V. MILLER, J. H. ADRAIR and A. S. BHALLA, *J. Mater. Res.* **8** (1993) 899.
29. C. P. BOWEN, A. S. BHALLA, R. E. NEWNHAM and C. A. RANDALL, *ibid.* **9** (1994) 781.
30. L. C. DAVIS, *J. Appl. Phys.* **72** (1992) 1334.
31. A. P. GAST and C. F. ZUKOSKI, *Adv. Coll. Interface Sci.* **30** (1989) 153.
32. S. FRADEN, A. J. HURD and R. B. MEYER, *Phys. Rev. Lett.* **63** (1989) 2373.

Received 14 August 1997
and accepted 22 April 1998